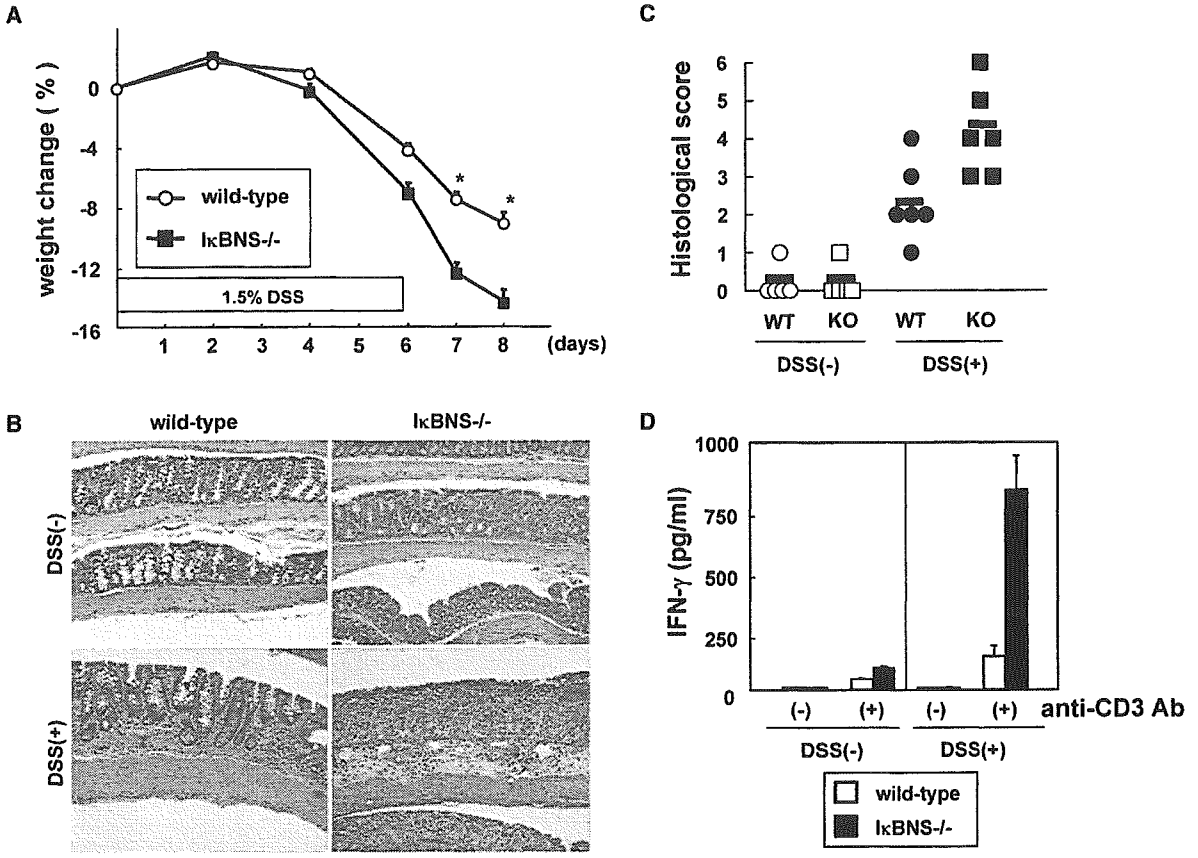

Figure 7. High Susceptibility to DSS Colitis in IκBNS$^{-/-}$ Mice

(A) Wild-type (n = 15) and IκBNS$^{-/-}$ mice (n = 15) were given 1.5% DSS in drinking water for 6 days and weighed everyday. Data are mean ± SD. *, $p < 0.05$.

(B) Histologic examination of the colons of wild-type and IκBNS$^{-/-}$ mice before or 9 days after initiation of DSS administration. H&E staining is shown. Representative of six mice examined. Magnification, 20×.

(C) The colitis scores shown for individual wild-type (circle) and IκBNS$^{-/-}$ mice (square) before (open) and after (closed) DSS treatment were total scores for individual sections as described in the Experimental Procedures section. Mean score for each group is also shown (black bar).

(D) CD4$^+$ T cells were purified from spleen of wild-type or IκBNS$^{-/-}$ mice either treated or nontreated with DSS. Then, CD4$^+$ T cells were cultured in the presence or absence of plate bound anti-CD3 Ab for 24 hr. Concentration of IFN-γ in the culture supernatants was measured by ELISA.

So far, characterized negative regulators are mainly involved in blockade of TLR signaling pathways in the cytoplasm or on the cell membrane. Accordingly, these negative regulators globally inhibit TLR-dependent gene induction. The nuclear IκB protein IκBNS is unique in that this molecule negatively regulates induction of a set of TLR-dependent genes by directly affecting NF-κB activity in the nucleus. Thus, TLR-dependent innate immune responses are regulated through a variety of mechanisms.

IκBNS-mediated inhibition of a set of TLR-dependent genes is probably explained by recruitment of IκBNS to the specific promoters. IκBNS was recruited to the IL-6 promoter, but not to the TNF-α promoter. In addition, LPS-induced recruitment of p65 to the TNF-α promoter was observed within 1 hr, whereas p65 recruitment to the IL-6 promoter was observed late, indicating that NF-κB activity was differentially regulated at both promoters. NF-κB activity at the TNF-α promoter is regulated in an IκBNS-independent manner, whereas the activity at the IL-6 promoter was IκBNS-dependent. Indeed, p65 recruitment to the TNF-α promoter was observed similarly in wild-type and IκBNS$^{-/-}$ macrophages, but the recruitment to the IL-6 promoter was sustained in IκBNS$^{-/-}$ cells. Previous reports indicate that IκBNS selectively associates with p50 subunit of NF-κB and affects NF-κB DNA binding activity (Fiorini et al., 2002; Hirotani et al., 2005). Consistent with these observations, IκBNS$^{-/-}$ macrophages showed prolonged LPS-induced NF-κB DNA binding activity and nuclear localization of p65. Taken together, these findings indicate that IκBNS, which is rapidly induced by TLR stimulation, might be recruited to gene promoters through association with p50, and contribute to termination of NF-κB activity. Termination of NF-κB activity has been shown to be induced by IKKα-mediated degradation of promoter-bound p65 (Lawrence et al., 2005). However, consistent with a recent report, we were not able to detect LPS-induced degradation of p65 in peritoneal macrophages and bone marrow-derived macrophages (Li et al., 2005). However, we could detect LPS-induced p65 degradation in the RAW264.7 macrophage cell line. In these cells, when constitutively expressed IκBNS, LPS-induced p65 turnover was

accelerated, indicating that IκBNS is involved in the degradation of promoter-bound p65. In the case of the TNF-α promoter, it is possible that NF-κB activity is already terminated when IκBNS expression is induced, and therefore IκBNS is no longer recruited to the TNF-α promoter. Alternatively, an unidentified mechanism that regulates selective recruitment of IκBNS to gene promoters might exist. The mechanisms by which IκBNS is recruited to the specific promoters through association with p50 remain unclear and would be a subject of further investigation.

Analyses of IκBNS$^{-/-}$ mice further highlighted the in vivo functions of IκBNS in limiting systemic and intestinal inflammation. IκBNS$^{-/-}$ mice succumbed to systemic LPS-induced endotoxin shock possibly due to sustained production of several TLR-dependent gene products such as IL-6 and IL-12p40. Furthermore, IκBNS$^{-/-}$ mice are more susceptible to intestinal inflammation induced by disruption of the epithelial barrier. Abnormal activation of innate immune cells caused by deficiency of IL-10 or Stat3 leads to spontaneous development of colonic inflammation (Kobayashi et al., 2003; Kuhn et al., 1993; Takeda et al., 1999). IκBNS$^{-/-}$ mice did not develop chronic colitis spontaneously until 20 week-old of age (our unpublished data). In Stat3 mutant mice, TLR-dependent production of proinflammatory cytokines increased over 10-fold compared to wild-type cells, which might contribute to the spontaneous intestinal inflammation (Takeda et al., 1999). In IκBNS$^{-/-}$ mice, increase in TLR-dependent production of proinflammatory cytokines such as IL-6 and IL-12p40 was mild compared to Stat3 mutant mice. In this case, the colonic epithelial barrier might contribute to prevention of excessive inflammatory responses in IκBNS$^{-/-}$ mice. However, when the barrier function of epithelial cells was disrupted by administration of DSS, IκBNS$^{-/-}$ mice suffered from severe intestinal inflammation accompanied by enhanced Th1 responses. IκBNS was shown to be expressed in CD11b^{+} cells residing in the colonic lamina propria (Hirotani et al., 2005). Therefore, in the absence of IκBNS, exposure of innate immune cells to intestinal microflora might result in increased or sustained production of proinflammatory cytokines such as IL-12p40, which induces exaggerated intestinal inflammation and Th1 cell development. Thus, IκBNS is responsible for the prevention of uncontrolled inflammatory responses in vivo.

In this study, we have shown that IκBNS is a selective inhibitor of TLR-dependent genes possibly through termination of NF-κB activity. Furthermore, IκBNS was responsible for prevention of inflammation through inhibition of persistent proinflammatory cytokine production. Future study that discloses the precise molecular mechanisms by which the nuclear IκB protein selectively inhibits TLR-dependent genes will provide basis for the development of new therapeutic strategies to a variety of inflammatory diseases.

Experimental Procedures

Generation of IκBNS-Deficient Mice

The *Ikbns* gene consists of eight exons (Figure 1A). The targeting vector was designed to replace a 1.8 kb fragment containing exons 5–8 of the *Ikbns* gene with a neomycin-resistance gene (*neo*). A short arm and a long arm of the homology region from the E14.1 ES genome were amplified by PCR. A herpes simplex virus thymidine kinase gene (HSV-TK) was inserted into the 3′ end of the vector. After the targeting vector was electroporated into ES cells, G418 and ganciclovir doubly resistant clones were selected and screened for homologous recombination by PCR and verified by Southern blot analysis using the probe indicated in Figure 1A. Two independently identified targeted ES clones were microinjected into C57BL/6 blastocysts. Chimeric mice were mated with C57BL/6 female mice, and heterozygous F1 progenies were intercrossed to obtain IκBNS$^{-/-}$ mice. Mice from these independent ES clones displayed identical phenotypes. All animal experiments were conducted according to guidelines of Animal Care and Use Committee at Kyushu University.

Reagents

LPS (*E. coli* 055:B5) was purchased from Sigma. Peptidoglycan was from Fluca. Pam_3CSK_4, MALP-2, and imiquimod were from Invivogen. Antibodies against p65 (C-20; sc-372), p50 (H-119; sc-7178 or NLS; sc-114), c-Rel (C; sc-71), and RNA polymerase II (H-224; sc-9001) were purchased from Santa Cruz. Rabbit anti-IκBNS Ab was generated against synthetic peptide (1-MEDSLDTRLY PEPSLSQVC-18) corresponding to N-terminal region of mouse IκBNS (MBL, Nagoya, Japan), and anti-IκBNS serum was affinity-purified using a column containing peptide-conjugated Sepharose 4B.

Preparation of Macrophages and Dendritic Cells

For isolation of peritoneal macrophages, mice were intraperitoneally injected with 2 ml of 4% thioglycollate medium (Sigma). Peritoneal exudate cells were isolated from the peritoneal cavity 3 days post injection. Cells were incubated for 2 hr and washed three times with HBSS. Remaining adherent cells were used as peritoneal macrophages for the experiments. To prepare bone marrow-derived macrophages, bone marrow cells were prepared from femora and tibia and passed through nylon mesh. Then cells were cultured in RPMI 1640 medium supplemented with 10% FCS, 100 μM 2-ME, and 10 ng/ml M-CSF (GenzymeTechne). After 6–8 days, the cells were used as macrophages for the experiments. Bone marrow-derived DCs were prepared by culturing bone marrow cells in RPMI 1640 medium supplemented with 10% FCS, 100 μM 2-ME, and 10 ng/ml GM-CSF (GenzymeTechne). After 6 days, the cells were used as DCs.

Measurement of Cytokine Production

Peritoneal macrophages or DCs were stimulated with various TLR ligands for 24 hr. Culture supernatants were collected and analyzed for TNF-α, IL-6, IL-12p40, IL-12p70, or IL-10 production with enzyme-linked immunosorbent assay (ELISA). Mice were intravenously injected with 1 mg of LPS and bled at the indicated periods. Serum concentrations of TNF-α, IL-6, and IL-12p40 were determined by ELISA. ELISA kits were purchased from GenzymeTechne and R&D Systems. For measurement of IFN-γ, CD4^{+} T cells were purified from spleen cells using CD4 microbeads (Miltenyi Biotec) and stimulated by plate bound anti-CD3ε antibody (145-2C11, BD PharMingen) for 24 hr. Concentrations of IFN-γ in the supernatants were determined by ELISA (GenzymeTechne).

Quantitative Real-Time RT-PCR

Total RNA was isolated with TRIzol reagent (Invitrogen, Carlsbad, CA), and 2 μg of RNA was reverse transcribed using M-MLV reverse transcriptase (Promega, Madison, WI) and oligo (dT) primers (Toyobo, Osaka, Japan) after treatment with RQ1 DNase I (Promega). Quantitative real-time PCR was performed on an ABI 7700 (Applied Biosystems, Foster City, CA) using TaqMan Universal PCR Master Mix (Applied Biosystems). All data were normalized to the corresponding elongation factor-1α (EF-1α) expression, and the fold difference relative to the EF-1α level was shown. Amplification conditions were: 50°C (2 min), 95°C (10 min), 40 cycles of 95°C (15 s), and 60°C (60 s). Each experiment was performed independently at least three times, and the results of one representative experiment are shown. All primers were purchased from Assay on Demand (Applied Biosystems).

Electrophoretic Mobility Shift Assay

Macrophages were stimulated with 100 ng/ml LPS for the indicated periods. Then, nuclear proteins were extracted, and incubated with an end-labeled, double-stranded oligonucleotide containing an NF-κB binding site of the IL-6 promoter in 25 μl of binding buffer (10 mM HEPES-KOH, [pH 7.8], 50 mM KCl, 1 mM EDTA [pH 8.0], 5 mM $MgCl_2$ and 10% glycerol) for 20 min at room temperature and loaded on a native 5% polyacrylamide gel. The DNA-protein complexes were visualized by autoradiography.

Western Blotting

Cells were lysed with RIPA buffer (50 mM Tris-HCl [pH 7.5], 150 mM NaCl, 1% Triton X-100, 0.5% Na-deoxycholate) containing protease inhibitors (Complete Mini; Roche). The lysates were separated on SDS-PAGE and transferred to PVDF membrane. The membranes were incubated with anti-IκBα Ab, anti-ERK Ab, anti-p38 Ab, anti-JNK Ab (Santa Cruz Biotechnology), anti-phospho-p38 Ab, anti-phospho-ERK Ab, or anti-phospho-JNK Ab (Cell Signaling Technology). Bound Abs were detected with SuperSignal West Pico Chemiluminescent Substrate (Pierce).

Immunofluorescence Staining

Macrophages were stimulated with 100 ng/ml LPS for the indicated periods, washed with Tris-buffered saline (TBS), and fixed with 3.7% formaldehyde in TBS for 15 min at room temperature. After permeabilization with 0.2% Triton X-100, cells were washed with TBS and incubated with 10 ng/ml of a rabbit anti-p50 or anti-p65 Ab (Santa Cruz Biotechnology) in TBS containing 1% bovine serum albumin, followed by incubation with Alexa Fluor 594-conjugated goat anti-rabbit immunoglobulin G (IgG; Molecular Probes, Eugene, OR). To stain the nucleus, cells were cultured with 0.5 μg/ml 4, 6-diamidino-2-phenylindole (DAPI; Wako, Osaka, Japan). Stained cells were analyzed using an LSM510 model confocal microscope (Carl Zeiss, Oberkochem, Germany).

Chromatin Immunoprecipitation

Chromatin immunoprecipitation (ChIP) was performed essentially with a described protocol (Upstate Biotechnology, Lake Placid, NY). In brief, peritoneal macrophages from wild-type and $I\kappa BNS^{-/-}$ mice were stimulated with 100 ng/ml LPS for 1, 3, or 5 hr, and then fixed with formaldehyde for 10 min. The cells were lysed, sheared by sonication using Bioruptor (CosmoBio), and incubated overnight with specific antibody followed by incubation with protein A-agarose saturated with salmon sperm DNA (Upsate Biotechnology). Precipitated DNA was analyzed by quantitative PCR (35 cycles) using primers 5′- CCCCAGATTGCCACAGAATC -3′ and 5′- CCAGT GAGTGAAAGGGACAG -3′ for the TNF-α promoter and 5′- TGTGTG TCGTCTGTCATGCG-3′ and 5′- AGCTACAGACATCCCCAGTCTC -3′ for the IL-6 promoter.

Induction of DSS Colitis

Mice received 1.5% (wt/vol) DSS (40,000 kDa; ICN Biochemicals), ad libitum, in their drinking water for 6 days, then switched to regular drinking water. The amount of DSS water drank per animal was recorded and no differences in intake between strains were observed. Mice were weighed for the determination of percent weight change. This was calculated as: percentage weight change = (weight at day X-day 0/weight at day 0) × 100. Statistical significance was determined by paired Student's t test. Differences were considered to be statistically significant at $p < 0.05$.

Histological Analysis

Colon tissues were fixed in 4% paraformaldehyde, rolled up, and embedded in paraffin in a Swiss roll orientation such that the entire length of the intestinal tract could be identified on single sections. After sectioning, the tissues were dewaxed in ethanol, rehydrated, and stained hematoxylin and eosin to study histological changes after DSS-induced damage. Histological scoring was performed in a blinded fashion by a pathologist, with a combined score for inflammatory cell infiltration (score, 0–3) and tissue damage (score, 0–3) (Araki et al., 2005). The presence of occasional inflammatory cells in the lamina propria was assigned a value of 0; increased numbers of inflammatory cells in the lamina propria as 1; confluence of inflammatory cells, extending into the submucosa, as 2; and transmural extension of the infiltrate as 3. For tissue damage, no mucosal damage was scored as 0; discrete lymphoepithelial lesions were scored as 1; surface mucosal erosion or focal ulceration was scored as 2; and extensive mucosal damage and extension into deeper structures of the bowel wall were scored as 3. The combined histological score ranged from 0 (no changes) to 6 (extensive cell infiltration and tissue damage).

Supplemental Data

Supplemental Data include four figures and are available with this article online at http://www.immunity.com/cgi/content/full/24/1/41/DC1/.

Acknowledgments

We thank Y. Yamada, K. Takeda, M. Otsu, and N. Kinoshita for technical assistance; M. Yamamoto and S. Akira for providing us with reagents, P. Lee for critical reading of the manuscript, and M. Kurata for secretarial assistance. This work was supported by grants from the Special Coordination Funds of the Ministry of Education, Culture, Sports, Science and Technology; the Uehara Memorial Foundation; the Mitsubishi Foundation; the Takeda Science Foundation; the Tokyo Biochemical Research Foundation; the Kowa Life Science Foundation; the Osaka Foundation for Promotion of Clinical Immunology; and the Sankyo Foundation of Life Science.

Received: July 15, 2005
Revised: September 16, 2005
Accepted: November 16, 2005
Published: January 17, 2006

References

Akira, S., and Takeda, K. (2004). Toll-like receptor signalling. Nat. Rev. Immunol. *4*, 499–511.

Araki, A., Kanai, T., Ishikura, T., Makita, S., Uraushihara, K., Iiyama, R., Totsuka, T., Takeda, K., Akira, S., and Watanabe, M. (2005). MyD88-deficient mice develop severe intestinal inflammation in dextran sodium sulfate colitis. J. Gastroenterol. *40*, 16–23.

Beutler, B. (2004). Inferences, questions and possibilities in Toll-like receptor signalling. Nature *430*, 257–263.

Bjorkbacka, H., Kunjathoor, V.V., Moore, K.J., Koehn, S., Ordija, C.M., Lee, M.A., Means, T., Halmen, K., Luster, A.D., Golenbock, D.T., and Freeman, M.W. (2004). Reduced atherosclerosis in MyD88-null mice links elevated serum cholesterol levels to activation of innate immunity signaling pathways. Nat. Med. *10*, 416–421.

Boone, D.L., Turer, E.E., Lee, E.G., Ahmad, R.C., Wheeler, M.T., Tsui, C., Hurley, P., Chien, M., Chai, S., Hitotsumatsu, O., et al. (2004). The ubiquitin-modifying enzyme A20 is required for termination of Toll-like receptor responses. Nat. Immunol. *5*, 1052–1060.

Brint, E.K., Xu, D., Liu, H., Dunne, A., McKenzie, A.N., O'Neill, L.A., and Liew, F.Y. (2004). ST2 is an inhibitor of interleukin 1 receptor and Toll-like receptor 4 signaling and maintains endotoxin tolerance. Nat. Immunol. *5*, 373–379.

Burns, K., Janssens, S., Brissoni, B., Olivos, N., Beyaert, R., and Tschopp, J. (2003). Inhibition of interleukin 1 receptor/Toll-like receptor signaling through the alternatively spliced, short form of MyD88 is due to its failure to recruit IRAK-4. J. Exp. Med. *197*, 263–268.

Chuang, T.H., and Ulevitch, R.J. (2004). Triad3A, an E3 ubiquitin-protein ligase regulating Toll-like receptors. Nat. Immunol. *5*, 495–502.

Diehl, G.E., Yue, H.H., Hsieh, K., Kuang, A.A., Ho, M., Morici, L.A., Lenz, L.L., Cado, D., Riley, L.W., and Winoto, A. (2004). TRAIL-R as a negative regulator of innate immune cell responses. Immunity *21*, 877–889.

Divanovic, S., Trompette, A., Atabani, S.F., Madan, R., Golenbock, D.T., Visintin, A., Finberg, R.W., Tarakhovsky, A., Vogel, S.N., Belkaid, Y., et al. (2005). Negative regulation of Toll-like receptor 4 signaling by the Toll-like receptor homolog RP105. Nat. Immunol. *6*, 571–578.

Eriksson, U., Ricci, R., Hunziker, L., Kurrer, M.O., Oudit, G.Y., Watts, T.H., Sonderegger, I., Bachmaier, K., Kopf, M., and Penninger, J.M.

(2003). Dendritic cell-induced autoimmune heart failure requires cooperation between adaptive and innate immunity. Nat. Med. *9*, 1484–1490.

Fiorini, E., Schmitz, I., Marissen, W.E., Osborn, S.L., Touma, M., Sasada, T., Reche, P.A., Tibaldi, E.V., Hussey, R.E., Kruisbeek, A.M., et al. (2002). Peptide-induced negative selection of thymocytes activates transcription of an NF-kappa B inhibitor. Mol. Cell *9*, 637–648.

Fukao, T., Tanabe, M., Terauchi, Y., Ota, T., Matsuda, S., Asano, T., Kadowaki, T., Takeuchi, T., and Koyasu, S. (2002). PI3K-mediated negative feedback regulation of IL-12 production in DCs. Nat. Immunol. *3*, 875–881.

Hirotani, T., Lee, P.Y., Kuwata, H., Yamamoto, M., Matsumoto, M., Kawase, I., Akira, S., and Takeda, K. (2005). The nuclear IkappaB protein IkappaBNS selectively inhibits lipopolysaccharide-induced IL-6 production in macrophages of the colonic lamina propria. J. Immunol. *174*, 3650–3657.

Honda, K., Yanai, H., Negishi, H., Asagiri, M., Sato, M., Mizutani, T., Shimada, N., Ohba, Y., Takaoka, A., Yoshida, N., and Taniguchi, T. (2005). IRF-7 is the master regulator of type-I interferon-dependent immune responses. Nature *434*, 772–777.

Iwasaki, A., and Medzhitov, R. (2004). Toll-like receptor control of the adaptive immune responses. Nat. Immunol. *5*, 987–995.

Kawai, T., Adachi, O., Ogawa, T., Takeda, K., and Akira, S. (1999). Unresponsiveness of MyD88-deficient mice to endotoxin. Immunity *11*, 115–122.

Kinjyo, I., Hanada, T., Inagaki-Ohara, K., Mori, H., Aki, D., Ohishi, M., Yoshida, H., Kubo, M., and Yoshimura, A. (2002). SOCS1/JAB is a negative regulator of LPS-induced macrophage activation. Immunity *17*, 583–591.

Kisielow, P., Bluthmann, H., Staerz, U.D., Steinmetz, M., and von Boehmer, H. (1988). Tolerance in T-cell-receptor transgenic mice involves deletion of nonmature CD4+8+ thymocytes. Nature *333*, 742–746.

Kitajima, S., Takuma, S., and Morimoto, M. (1999). Changes in colonic mucosal permeability in mouse colitis induced with dextran sulfate sodium. Exp. Anim. *48*, 137–143.

Kobayashi, K., Hernandez, L.D., Galan, J.E., Janeway, C.A., Jr., Medzhitov, R., and Flavell, R.A. (2002). IRAK-M is a negative regulator of Toll-like receptor signaling. Cell *110*, 191–202.

Kobayashi, M., Kweon, M.N., Kuwata, H., Schreiber, R.D., Kiyono, H., Takeda, K., and Akira, S. (2003). Toll-like receptor-dependent production of IL-12p40 causes chronic enterocolitis in myeloid cell-specific Stat3-deficient mice. J. Clin. Invest. *111*, 1297–1308.

Kuhn, R., Lohler, J., Rennick, D., Rajewsky, K., and Muller, W. (1993). Interleukin-10-deficient mice develop chronic enterocolitis. Cell *75*, 263–274.

Kuwata, H., Watanabe, Y., Miyoshi, H., Yamamoto, M., Kaisho, T., Takeda, K., and Akira, S. (2003). IL-10-inducible Bcl-3 negatively regulates LPS-induced TNF-alpha production in macrophages. Blood *102*, 4123–4129.

Lang, K.S., Recher, M., Junt, T., Navarini, A.A., Harris, N.L., Freigang, S., Odermatt, B., Conrad, C., Ittner, L.M., Bauer, S., et al. (2005). Toll-like receptor engagement converts T-cell autoreactivity into overt autoimmune disease. Nat. Med. *11*, 138–145.

Lawrence, T., Bebien, M., Liu, G.Y., Nizet, V., and Karin, M. (2005). IKKalpha limits macrophage NF-kappaB activation and contributes to the resolution of inflammation. Nature *434*, 1138–1143.

Leadbetter, E.A., Rifkin, I.R., Hohlbaum, A.M., Beaudette, B.C., Shlomchik, M.J., and Marshak-Rothstein, A. (2002). Chromatin-IgG complexes activate B cells by dual engagement of IgM and Toll-like receptors. Nature *416*, 603–607.

Li, Q., Lu, Q., Bottero, V., Estepa, G., Morrison, L., Mercurio, F., and Verma, I.M. (2005). Enhanced NF-(kappa)B activation and cellular function in macrophages lacking I(kappa)B kinase 1 (IKK1). Proc. Natl. Acad. Sci. USA *102*, 12425–12430.

Liew, F.Y., Xu, D., Brint, E.K., and O'Neill, L.A. (2005). Negative regulation of Toll-like receptor-mediated immune responses. Nat. Rev. Immunol. *5*, 446–458.

Michelsen, K.S., Wong, M.H., Shah, P.K., Zhang, W., Yano, J., Doherty, T.M., Akira, S., Rajavashisth, T.B., and Arditi, M. (2004). Lack of Toll-like receptor 4 or myeloid differentiation factor 88 reduces atherosclerosis and alters plaque phenotype in mice deficient in apolipoprotein E. Proc. Natl. Acad. Sci. USA *101*, 10679–10684.

Moore, K.W., de Waal Malefyt, R., Coffman, R.L., and O'Garra, A. (2001). Interleukin-10 and the interleukin-10 receptor. Annu. Rev. Immunol. *19*, 683–765.

Motoyama, M., Yamazaki, S., Eto-Kimura, A., Takeshige, K., and Muta, T. (2005). Positive and negative regulation of nuclear factor-kappaB-mediated transcription by IkappaB-zeta, an inducible nuclear protein. J. Biol. Chem. *280*, 7444–7451.

Nakagawa, R., Naka, T., Tsutsui, H., Fujimoto, M., Kimura, A., Abe, T., Seki, E., Sato, S., Takeuchi, O., Takeda, K., et al. (2002). SOCS-1 participates in negative regulation of LPS responses. Immunity *17*, 677–687.

Natoli, G., Saccani, S., Bosisio, D., and Marazzi, I. (2005). Interactions of NF-kappaB with chromatin: the art of being at the right place at the right time. Nat. Immunol. *6*, 439–445.

Pasare, C., and Medzhitov, R. (2004). Toll-dependent control mechanisms of CD4 T cell activation. Immunity *21*, 733–741.

Saccani, S., Marazzi, I., Beg, A.A., and Natoli, G. (2004). Degradation of promoter-bound p65/RelA is essential for the prompt termination of the nuclear factor kappaB response. J. Exp. Med. *200*, 107–113.

Sakaguchi, S., Negishi, H., Asagiri, M., Nakajima, C., Mizutani, T., Takaoka, A., Honda, K., and Taniguchi, T. (2003). Essential role of IRF-3 in lipopolysaccharide-induced interferon-beta gene expression and endotoxin shock. Biochem. Biophys. Res. Commun. *306*, 860–866.

Strober, W., Fuss, I.J., and Blumberg, R.S. (2002). The immunology of mucosal models of inflammation. Annu. Rev. Immunol. *20*, 495–549.

Takaoka, A., Yanai, H., Kondo, S., Duncan, G., Negishi, H., Mizutani, T., Kano, S., Honda, K., Ohba, Y., Mak, T.W., and Taniguchi, T. (2005). Integral role of IRF-5 in the gene induction programme activated by Toll-like receptors. Nature *434*, 243–249.

Takeda, K., Clausen, B.E., Kaisho, T., Tsujimura, T., Terada, N., Forster, I., and Akira, S. (1999). Enhanced Th1 activity and development of chronic enterocolitis in mice devoid of Stat3 in macrophages and neutrophils. Immunity *10*, 39–49.

Wald, D., Qin, J., Zhao, Z., Qian, Y., Naramura, M., Tian, L., Towne, J., Sims, J.E., Stark, G.R., and Li, X. (2003). SIGIRR, a negative regulator of Toll-like receptor-interleukin 1 receptor signaling. Nat. Immunol. *4*, 920–927.

Wessells, J., Baer, M., Young, H.A., Claudio, E., Brown, K., Siebenlist, U., and Johnson, P.F. (2004). BCL-3 and NF-kappaB p50 attenuate lipopolysaccharide-induced inflammatory responses in macrophages. J. Biol. Chem. *279*, 49995–50003.

Yamamoto, M., Sato, S., Hemmi, H., Hoshino, K., Kaisho, T., Sanjo, H., Takeuchi, O., Sugiyama, M., Okabe, M., Takeda, K., and Akira, S. (2003). Role of adaptor TRIF in the MyD88-independent toll-like receptor signaling pathway. Science *301*, 640–643.

Yamamoto, M., Yamazaki, S., Uematsu, S., Sato, S., Hemmi, H., Hoshino, K., Kaisho, T., Kuwata, H., Takeuchi, O., Takeshige, K., et al. (2004). Regulation of Toll/IL-1-receptor-mediated gene expression by the inducible nuclear protein IkappaBzeta. Nature *430*, 218–222.

CCR7 Is Critically Important for Migration of Dendritic Cells in Intestinal Lamina Propria to Mesenteric Lymph Nodes[1]

Myoung Ho Jang,[2]* Nagako Sougawa,[2]* Toshiyuki Tanaka,* Takako Hirata,† Takachika Hiroi,‡ Kazuo Tohya,§ Zijin Guo,* Eiji Umemoto,* Yukihiko Ebisuno,* Bo-Gie Yang,* Ju-Young Seoh,¶ Martin Lipp,‖ Hiroshi Kiyono,‡ and Masayuki Miyasaka[3]*

Although dendritic cells (DCs) located in the small intestinal lamina propria (LP-DCs) migrate to mesenteric lymph nodes (MLNs) constitutively, it is unclear which chemokines regulate their trafficking to MLNs. In this study we report that LP-DCs in unperturbed mice require CCR7 to migrate to MLNs. In vitro, LP-DCs expressing CCR7 migrated toward CCL21, although the LP-DCs appeared morphologically and phenotypically immature. In MLNs, DCs bearing the unique LP-DC phenotype ($CD11c^{high}CD8\alpha^{int}CD11b^{low}\alpha_L^{low}\beta_7^{high}$ and $CD11c^{high}CD8\alpha^{-}CD11b^{high}\alpha_L^{low}\beta_7^{high}$) were abundant in wild-type mice, but were markedly fewer in CCL19-, CCL21-Ser-deficient *plt/plt* mice and were almost absent in CCR7-deficient mice, indicating the critical importance of CCR7 in LP-DC trafficking to MLNs. Interestingly, $CCR7^+$ DCs in MLNs with the unique LP-DC phenotype had numerous vacuoles containing cellular debris in the cytoplasm, although MLN-DCs themselves were poorly phagocytic, suggesting that the debris was derived from the LP, where the LP-DCs ingested apoptotic intestinal epithelial cells (IECs). Consistent with this, LP-DCs ingested IECs vigorously in vitro. By presenting IEC-associated Ag, the LP-DCs also induce T cells to produce IL-4 and IL-10. Collectively, these results strongly suggest that LP-DCs with unique immunomodulatory activities migrate to MLNs in a CCR7-dependent manner to engage in the presentation of IEC-associated Ags acquired in the LP. *The Journal of Immunology,* **2006, 176: 803–810.**

Dendritic cells (DCs)[4] are cardinal constituents of the immune system and play pivotal roles in the induction of Ag-specific immune responses and the maintenance of self-tolerance (1). DCs are abundant in the small intestine, both in organized lymphoid tissues (Peyer's patches (PPs) and isolated lymphoid follicles (ILFs)) and in the lamina propria (LP), the layer of connective tissue between the epithelium and the muscularis mucosa, where they act as sentinels for incoming Ags. The precise discrimination between harmless Ags and dangerous pathogens by these DCs is a likely key mechanism for the maintenance of gut immune homeostasis (2).

Among the intestinal DCs, the DC subsets in PPs have been characterized in the most detail (3–6). PP-DCs can educate Ag-specific T cells to produce IL-4 and IL-10 (3) and confer gut-homing specificity on T cells (7, 8), indicating that they have unique immune-inductive abilities. In contrast, LP-DCs have been only incompletely characterized, mainly due to difficulty in isolating them. Recent investigations have revealed, however, that LP-DCs of a certain subset extend dendrites in a CX_3CR1-dependent manner to the luminal side of the gut for the uptake of Ags (9, 10). In addition, LP-DCs that reside in the terminal ileum sample commensal bacteria and constitutively express IL-12 p40, indicating that these LP-DCs may be involved in the predisposition to chronic inflammation (11). LP-DCs may also be important in the presentation of bacterial Ags directly to LP B cells (12, 13). LP-DCs obtained from mice treated with Flt3 (FMS-like tyrosine kinase 3) ligand, express high levels of IL-10 and type I IFN and can induce a state of immune hyporesponsiveness upon in vivo transfer (14), suggesting that LP-DCs may have an immunomodulatory role in the gut.

Apart from the LP-DCs, a distinct DC subset has been documented in rat intestinal lymph that can constitutively endocytose apoptotic intestinal epithelial cells (IECs) and transport them to the T cell areas of mesenteric lymph nodes (MLNs). However, it remains unclear whether these DCs are derived from the LP, PPs, and/or other intestinal compartment(s). In addition, their function remains unexplored, although they have been implicated in tolerance induction (15). It has been separately reported that among DCs in the MLNs, the $CD8\alpha^{-}CD11b^{+}$ DC subset plays a critical role in inducing cross-tolerance to food Ags, although it remains to be determined whether these DCs take up dying IECs (16).

DCs are thought to leave peripheral tissues when they receive an inflammatory or danger signal. During this process, DCs begin to mature, and the expression of CCR7 increases (17–19), which allows the DCs to enter lymph vessels and gain access to T cell areas

*Laboratory of Immunodynamics, Department of Microbiology and Immunology, Osaka University Graduate School of Medicine, and †21st Century Center of Excellence Program, Research Institute for Microbial Diseases, Osaka University, Osaka, Japan; ‡Division of Mucosal Immunology, Institute of Medical Science, University of Tokyo, Tokyo, Japan; §Department of Anatomy, Kansai College of Oriental Medicine, Osaka, Japan; ¶Department of Microbiology, College of Medicine, Ewha Woman's University, Seoul, Korea; and ‖Max Delbrück Center for Molecular Medicine, Berlin, Germany

Received for publication September 12, 2005. Accepted for publication October 28, 2005.

The costs of publication of this article were defrayed in part by the payment of page charges. This article must therefore be hereby marked *advertisement* in accordance with 18 U.S.C. Section 1734 solely to indicate this fact.

[1] This work was supported by a Grant-in-Aid from the Ministry of Education, Culture, Sports, Science, and Technology of Japan, and a grant for Advanced Research on Cancer from the Ministry of Education, Culture, Sports, Science, and Technology of Japan.

[2] M.H.J. and N.S. contributed equally to this work.

[3] Address correspondence and reprint requests to Dr. Masayuki Miyasaka, Laboratory of Immunodynamics, Department of Microbiology and Immunology, Osaka University Graduate School of Medicine, C8, 2-2 Yamada-oka, Suita 565-0871, Japan. E-mail address: mmiyasak@orgctl.med.osaka-u.ac.jp

[4] Abbreviations used in this paper: DC, dendritic cell; IEC, intestinal epithelial cell; ILF, isolated lymphoid follicle; LN, lymph node; LP, lamina propria; MLN, mesenteric lymph node; PP, Peyer's patch; SP-DC, splenic DC.

0022-1767/06/$02.00

in draining lymph nodes (LNs) in a CCR7-dependent manner (20). Corroborating this, a deficiency of CCR7 or its ligands, CCL19 and CCL21, leads to impaired DC migration into draining LNs and abnormal lymph node architecture in peripheral tissues (21, 22). In addition, a recent study indicates that steady-state trafficking of skin DCs to the draining LNs in peripheral tissues is also regulated by CCR7-mediated signaling (23). However, it is not known whether this commonly held paradigm of DC trafficking being driven by CCR7-mediated signaling holds true for DCs in the intestinal compartment as well.

In the present study we found that there are at least two LP-DC subsets in the intestinal LP of unperturbed mice and that they both require CCR7 for their constitutive migration to the MLNs. They vigorously ingest apoptotic IECs and, hence, are likely to correspond to the cells identified by Huang et al. (15) in rat mesenteric lymph. As suggested previously (15), LP-DCs can present IEC-associated Ags to $CD4^+$ T cells, inducing their differentiation into IL-4- and IL-10-producing cells. These results strongly indicate that LP-DCs bearing a unique immunomodulatory activity migrate constitutively to MLNs in a CCR7-dependent manner, thus generating a noninflammatory environment in the MLNs.

Materials and Methods

Mice

BALB/c mice were obtained from CLEA Japan. C57BL/6 mice were obtained from Japan SLC. Mice transgenic for a TCR that recognizes the $OVA_{323-339}$ peptide in the context of $I\text{-}A^d$ (DO 11.10 TCR-$\alpha\beta$ transgenic mice) on the BALB/c background were a gift from Dr. S. Ono (Osaka University Graduate School of Medicine, Osaka, Japan). The *plt/plt* mice on the B6 background were provided by Dr. H. Nakano (Duke University Medical Center, Raleigh, NC). CCR7-deficient mice on the C57BL/6 background were produced as previously described (21). All animal experiments were performed under an experimental protocol approved by the ethics review committee for animal experimentation of Osaka University Graduate School of Medicine.

Preparation of DCs from small intestinal LP, PPs, MLNs, and spleen

Small intestinal segments and PPs were treated with PBS containing 10% FCS, 20 mM HEPES, 100 U/ml penicillin, 100 μg/ml streptomycin, 1 mM sodium pyruvate, 10 mM EDTA, and 10 μg/ml polymyxin B (Calbiochem) for 30 min at 37°C to remove epithelial cells and were washed extensively with PBS. Small intestinal segments, PPs, MLNs, and spleen were digested with 400 Mandl units/ml collagenase D (Roche) and 10 μg/ml DNase I (Roche) in RPMI 1640/10% FCS with continuous stirring at 37°C for 45–90 min. EDTA was added (10 mM final concentration), and the cell suspension was incubated for an additional 5 min at 37°C. Cells were spun through a 15.5% Accudenz (Accurate Chemical & Scientific) solution to enrich for DCs. The obtained cells were incubated with FITC-conjugated anti-CD11b and PE-conjugated anti-CD11c after FcR blocking. DC subsets were sorted on the basis of their expression of CD11c and CD11b by FACSVantage SE (BD Biosciences). The purity of the sorted DCs was routinely >95%. For the morphological study, cytospin preparations from purified DC subsets were stained with May-Grunwald-Giemsa solution.

Double immunofluorescence staining of small intestinal LP

To determine the location of LP-DCs in the small intestinal LP, biotinylated anti-CD11c and FITC-conjugated anti-CD11b mAbs were applied overnight at 4°C to sections cut from frozen tissue. Samples were washed and then incubated with streptavidin-Alexa 594 (Molecular Probes) for 2 h at room temperature. To detect $CCR7^+$ DCs in the small intestinal LP, frozen sections of the small intestine were stained with rabbit anti-mouse CCR7 pAb, provided by Dr. K. Matsushima (University of Tokyo School of Medicine, Tokyo, Japan) and biotinylated anti-CD11c mAb overnight at 4°C. The sections were washed and then further incubated with Alexa 488-conjugated chicken anti-rabbit IgG Ab (Molecular Probes) and streptavidin-Alexa 594 for 2 h at room temperature. Immunohistochemical staining was analyzed with a Radiance 2100/Bio-Rad confocal laser microscope (Bio-Rad).

Flow cytometry

Fluorochrome-conjugated anti-CD11c (HL3), anti-CD11b (M1/70), and anti-CD8α (53-6.7) mAbs were used for DC staining. Anti-mouse CD16/CD32 (2.4G2) was used for FcR blocking. The expression of integrins was determined using mAbs to integrin α_L (CD11a; M17/4) and β_7 (M293). The expression of costimulatory molecules was determined using mAbs to B7-1 (CD80; 16-10A1), B7-2 (CD86; GL1), CD40 (3/23), and $I\text{-}A^d$ (AMS-32.1). These reagents were all purchased from BD Pharmingen. After the FcRs were blocked for 15 min at 4°C, the cells were stained for integrins, CD8α, CD11c, CD11b, and costimulatory molecules and then analyzed with a FACSCalibur (BD Biosciences). The DCs were identified by gating on the $CD11c^{high}$ cells. CCR7 expression by DCs was determined using the CCL19-Fc chimeric protein provided by Drs. K. Hieshima and O. Yoshie (Kinki University School of Medicine, Kinki, Japan).

RT-PCR for chemokine receptor expression

Total RNA was prepared from freshly isolated LP-DC using TRIzol (Invitrogen Life Technologies). RT of total RNA was conducted using oligo$(dT)_{18}$ primer and SensiScript reverse transcriptase (Qiagen). PCR was conducted using primer pairs for CCR1 (sense, AGAAGCCTACCCCA CAAC; antisense, TGGCCAGGTATCTGTCAA), CCR7 (sense, GGTGT GCCTCTGCCAAGA; antisense, TGCCAAAGATGCCCTTAC), CCR9 (sense, TGCTACTGGAGACAACTTCG; antisense, CTCCTCAGAACT GCAGTTAC), and β-actin (sense, ATGGATGACGATATCGCT; antisense, ATGAGGTAGTCTGTCAGGT) and Ex-*Taq* polymerase (Takara Shuzo). The PCR conditions were 30 cycles at 97, 57, and 72°C for 30 s each, and the products were analyzed on agarose gels.

Chemotaxis assays

All cell suspensions and chemokine dilutions were made in RPMI 1640 containing 0.5% low endotoxin BSA (Sigma-Aldrich). The chemokine CCL21 was purchased from Techne. Chemotactic assays were performed as previously described (24). Two hours after the start of migration, the inserts were removed. Migrated DCs were identified on a FACSCalibur using FITC-conjugated anti-CD11b mAb and PE-conjugated anti-CD11c mAb.

Real-time chemotaxis assay

Real-time chemotaxis assays were performed as previously described (25). To count the migrated cells in each channel, images of the cells in each channel were digitally recorded onto a computer hard disk with time-lapse intervals of 60 s.

Detection of apoptotic IECs in MLN-DCs

To detect IECs-derived apoptotic DNA in DCs, cytospin preparations from FACS-sorted MLN-DCs were fixed with 1% paraformaldehyde and stained using an ApopTag peroxidase in situ apoptosis detection kit (Serologicals) Detection of alkaline phosphatase activity in the FACS-sorted $CD11c^{high}CD8\alpha^{int}\alpha_L{}^{low}\beta_7{}^{high}$ MLN-DC subset was performed using the Vector Red Alkaline Phosphatase Substrate Kit I (Vector Laboratories).

Electron microscopy

Isolated cells were spun at 400 × *g* and fixed in 1% in glutaraldehyde in 0.1 M phosphate buffer for 1 h at 4°C. After being washed, the cells were embedded in 2% agarose gel and postfixed in 2% osmium tetroxide in 0.1 M phosphate buffer for 2 h at 4°C. The fixed samples were then dehydrated in a graded ethanol series, infiltrated with propylene oxide, and embedded in Quetol 812 epoxy resin. Ultrathin sections were stained with 2% uranyl acetate and Reynold's lead citrate, then examined using a JEOL JEM-1230 electron microscope.

In vitro uptake of CFSE-labeled apoptotic epithelial cells by DCs

Small IECs were obtained as described previously (26). IECs were then labeled with CFSE (Molecular Probes) at a concentration of 5 μM for 5 min at 37°C and cultured for 4 h to induce spontaneous apoptosis. Enriched DCs were mixed with CFSE-labeled apoptotic IECs and cultured for 4 h at 37°C. After the coculture, cells were stained with PE-conjugated anti-CD11c mAb and allophycocyanin-conjugated anti-CD11b mAb to identify the DC subsets. The uptake of apoptotic IECs by DCs was evaluated by FACSCalibur.

Analysis of $CD4^+$ T cell proliferation and cytokine production

IECs obtained as described above were loaded with OVA (Sigma-Aldrich) by osmotic shock (27). They were then cocultured with DCs for 4 h, and

the DC subsets were subsequently sorted on the basis of their expression of CD11c and CD11b. Purified DCs (5×10^3) and DO11.10 OVA TCR-transgenic T cells (1×10^5) were mixed in 96-well plates (1/20). After 7 days, the cells were collected and stained with anti-mouse DO11.10 TCR (KJ1-26; Caltag Laboratories) and anti-mouse CD4 (RM4-5) mAbs. Dead cells were excluded using 7-aminoactinomycin D (Sigma-Aldrich). T cell proliferation was measured by CFSE dilution. To examine cytokine secretion, DO11.10 $CD4^+$ T cells were cocultured with IEC-OVA-containing DCs for 14 days (two-round stimulation with IEC-OVA-containing DCs with a 7-day interval). The T cells were then washed and restimulated for 6 h with anti-CD3 mAb in the presence of monensin (BD Pharmingen). Intracellular cytokine staining was performed according to the manufacturer's instructions (BD Pharmingen).

Results

Small intestinal LP contains two distinct DC subsets

We first determined the localization of LP-DC subsets in the small intestine by immunohistochemistry. As shown in Fig. 1*A*, cells that were $CD11b^-/CD11c^+$ (open arrowheads) and $CD11b^+/CD11c^+$ (filled arrowheads) were readily recognizable in the LP, indicating that the small intestinal LP contains at least two phenotypically distinguishable DC subsets.

We next attempted to isolate LP-DCs and successfully obtained substantial numbers of low density leukocytes from the LP ($1.95 \pm 0.5 \times 10^6$ cells/mouse; $n = 34$), of which the $CD11c^+$ DCs constituted ~10–15%. Among these cells, at least two LP-DC subsets could be recognized on the basis of their different CD11c/CD11b expression patterns: $CD11c^{high}CD11b^{low}$ (R1; 4.9 ± 2.0% of low density cells) and $CD11c^{high}CD11b^{high}$ (R2; 8.4 ± 2.0%; Fig. 1*B*). The remaining cells, which were $CD11c^{int}CD11b^{high}$, consisted mainly of cells that contained eosinophilic granules (J.-H. Seoh and M. H. Jang, manuscript in preparation). The $CD11c^{high}$ LP-DC subsets were heterogeneous in their $CD8\alpha$ expression, in that the $CD11c^{high}CD11b^{low}$ subset expressed $CD8\alpha$ at an intermediate level ($CD8\alpha^{int}$), whereas the $CD11c^{high}CD11b^{high}$ subset was $CD8\alpha^-$ (Fig. 1*B*). Thus, the phenotypes of the R1 and R2 subsets were $CD11c^{high}CD8\alpha^{int}CD11b^{low}$ and $CD11c^{high}CD8\alpha^-CD11b^{high}$, respectively.

These two subsets were found not only in the intestines of $Id2^{-/-}$ mice, which are completely deficient in PPs and ILFs (28), but also in the BALB/c small intestine from which PPs and ILFs had been surgically removed before the isolation procedure (data not shown), suggesting that they are indeed derived from the small intestinal LP and not PPs or ILFs. Interestingly, the freshly isolated R1 and R2 subsets both had few dendrites. The nuclear chromatin was not very condensed, and the cytoplasm was light blue to grayish when stained with May-Grunwald-Giemsa solution, suggesting that the LP-DCs were not fully mature (Fig. 1*C*).

The expression of costimulatory molecules also supported the idea that these cells were somewhat immature. As shown in Fig. 1*D*, LP-DCs showed substantially lower expression of MHC class II and CD40 than DCs from PPs and MLNs, indicating that they were less mature than other DCs in the intestinal compartment. Interestingly, however, the LP-DCs displayed a relatively high expression level of B7-2, as seen in PP-DCs, if not as high as that expressed by MLN-DCs, indicating that the LP-DCs may not be entirely immature but, rather, may constitute semimature subsets. The $CD11c^{high}$ LP-DC subsets were $DEC\text{-}205^+$, but $B220^-$ and $Gr\text{-}1^-$ (data not shown), indicating that they are distinct from plasmacytoid DCs (29) or the recently identified $CD70^+$ APCs (30) in the LP, both of which express readily detectable levels of DEC-205, B220, and Gr-1.

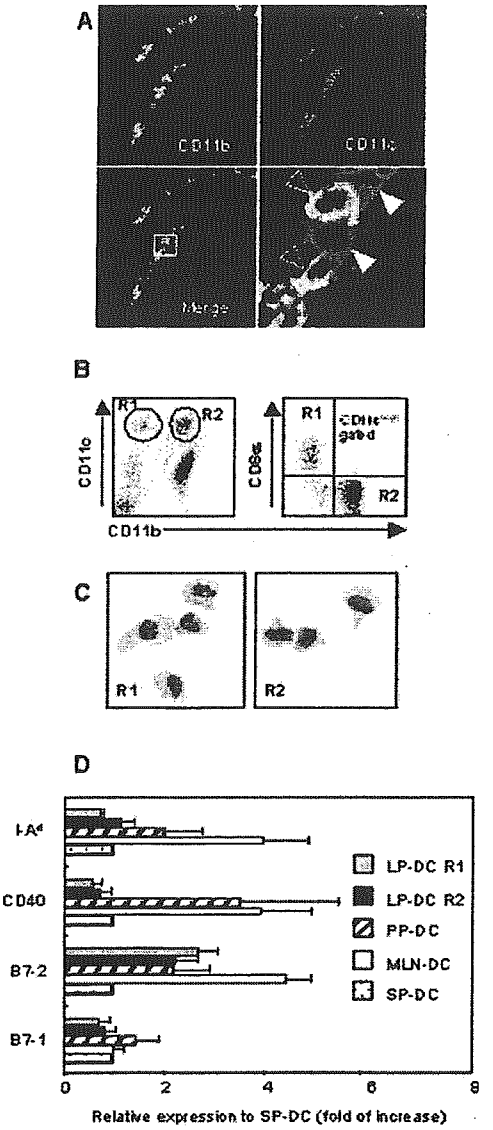

FIGURE 1. Identification of two DC subpopulations in the LP of the small intestine. *A*, Frozen sections of small intestine were fixed, stained with Abs specific for CD11b (green) and CD11c (red), and analyzed by confocal microscopy. Two cell subsets, $CD11b^-CD11c^+$ (red; open arrowheads) and $CD11b^+CD11c^+$ (yellow; filled arrowheads) were readily identifiable within the LP. *B*, Low density lamina propria cells were isolated from the small intestines of BALB/c mice and spun through a 15.5% Accudenz gradient. Enriched DCs were stained for $CD8\alpha$, CD11b, and CD11c and analyzed by flow cytometry. *C*, Two DC subsets (R1 ($CD11c^{high}CD8\alpha^{int}CD11b^{low}$) and R2 ($CD11c^{high}CD8\alpha^-CD11b^{high}$)) were FACS-sorted based on their CD11c and CD11b expressions and stained with May-Grunwald-Giemsa. The R1 and R2 subsets had a morphology associated with highly motile cells. *D*, The LP-DC subsets had a semimature phenotype. DC subsets from LP, PPs, MLNs, and spleen (SP) were stained for CD11c, CD11b, and B7-1, B7-2, CD40, or $I\text{-}A^d$ and analyzed by flow cytometry. The expression levels are shown as the ratio of the mean fluorescence intensity (MFI) to the fluorescence intensity of SP-DCs.

LP-DC subsets express CCR7 and show directional migration toward CCL21

Although steady-state trafficking of DCs from the skin to the draining LNs is regulated by CCR7-mediated signaling (23), it remains to be established whether LP-DC trafficking is also regulated by a

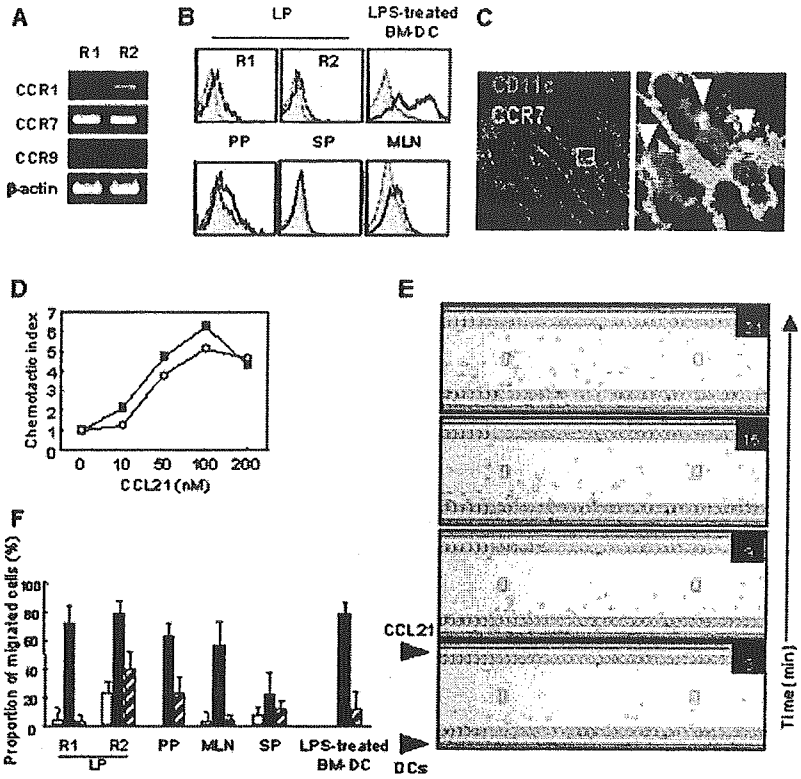

FIGURE 2. LP-DC subsets express CCR7 and show directional migration toward CCL21. *A*, Expression of CCR7 mRNA. cDNA was prepared from total RNA obtained from freshly FACS-sorted LP-DCs, and the expression of chemokine receptors was analyzed by semiquantitative PCR. *B*, Expression of CCR7 protein on the cell surface. DCs were stained for CCR7 using the CCL19-Fc chimera protein (□). LPS-stimulated bone marrow-derived DC was used as a positive control, and human Ig Fc protein served as a negative control (▨). *C*, Localization of $CCR7^+/CD11c^+$ DCs in the small intestinal LP. Frozen sections of the small intestine were fixed and stained with anti-CCR7 pAb and biotinylated anti-CD11c mAb. The sections were further incubated with Alexa 488-conjugated secondary Ab and streptavidin-Alexa 594. Arrows indicate $CCR7^+/CD11c^+$ cells. *D*, Chemotaxis analysis by Transwell. LP-DCs were placed in the upper well of a Transwell apparatus (5-μm pore size), and an increasing concentration of CCL21 was added to the lower well for 2 h. The migrated cells were stained for CD11c and CD11b, then analyzed by FACSCalibur. The proportion of migrated cells in each population was calculated as a fraction of the input population. The chemotactic index is shown as the ratio of the proportion of cells that migrated in the presence of chemokine to the proportion that migrated in the absence of chemokine. ■, R1 subset; ○, R2 subset. *E*, Time-lapse video monitoring of chemotaxis. Isolated LP-DCs were applied to the microchemotaxis chamber. After aligning the cells on the edge of the microchannel of the chamber, CCL21 (10 μM) was applied to the opposite side of the microchannel (see *top* of each frame), so that a concentration gradient of the chemokine formed from the top to the bottom of the channel. The migration of cells in the microchannel was subsequently monitored at 6-min intervals. Note that a significant fraction of the cells had begun migrating from the bottom to the top of the field 15–21 min after the addition of CCL21. *F*, Quantitative evaluation of chemotactic responses to CCL21. Data are shown as the proportion of cells that migrated across the microchannel to the total cells in the assay area. □, Medium alone; ■, CCL21; ▨, CCL21 with PTX treatment. The data are representative of at least three independent experiments.

CCR7-dependent mechanism. We thus examined CCR7 expression in LP-DCs. In the R1 ($CD11c^{high}CD11b^{low}$) and R2 ($CD11c^{high}CD11b^{high}$) subsets, CCR7 mRNA was highly expressed, whereas CCR9 mRNA was absent (Fig. 2*A*). Consistent with this, LP-DCs were $CCR7^+$, as evidenced by their binding of a CCL19-fusion protein (Fig. 2*B*), and $CD11c^+$ DCs expressing CCR7 were readily detectable in the LP by immunohistochemistry (Fig. 2*C*). Furthermore, in vitro, the $CD11c^{high}$ LP-DCs efficiently migrated through Transwell inserts in response to CCL21 with the typical bell-shaped dose-response curve that is characteristic of chemotaxis (Fig. 2*D*). To verify that this reflects directional, but not random, migration, we adopted an optical chemotaxis assay system that allows time-lapse video monitoring of cell behavior in silicon-coated microchannels (25). As shown in Fig. 2*E* and supplemental movie A,[5] LP-DCs moved swiftly along the CCL21 concentration gradient, verifying that they can migrate directionally toward a CCL21 source as a result of expressing functional CCR7. Compared with DCs from other tissues, LP-DCs showed much stronger chemotaxis toward CCL21 than splenic DCs (SP-DCs), but their chemotaxis was comparable to that seen in MLN-DCs and PP-DCs (Fig. 2*F*). LPS-stimulated, bone marrow-derived DCs responded to CCL21 much like the LP-DC subsets. In all these cell types, CCL21-mediated migration was significantly blocked by pertussis toxin. These data indicate that LP-DCs with relatively immature morphology and phenotype can migrate toward CCL21 as efficiently as mature DCs without deliberate inflammatory stimulation.

LP-DCs migrate to MLNs in a CCR7-dependent manner

We next investigated whether LP-DCs could be identified in the MLNs and, if so, whether their migration was dependent on CCR7. Because a recent study indicated that DC migrants to lymph nodes could be discriminated by their surface phenotype (31), we first compared the expressions of various surface markers on the $CD11c^{high}$ DCs obtained from the LP, PPs, MLNs, and spleen. As shown in Fig. 3*A*, LP-DCs highly expressed β_7 integrin compared with other DCs. In this regard, LP-DCs contained $CD8\alpha^{int}\beta_7^{high}$ and $CD8\alpha^-\beta_7^{high}$ subpopulations, which correspond to the R1 and

[5] The online version of this article contains supplemental material.

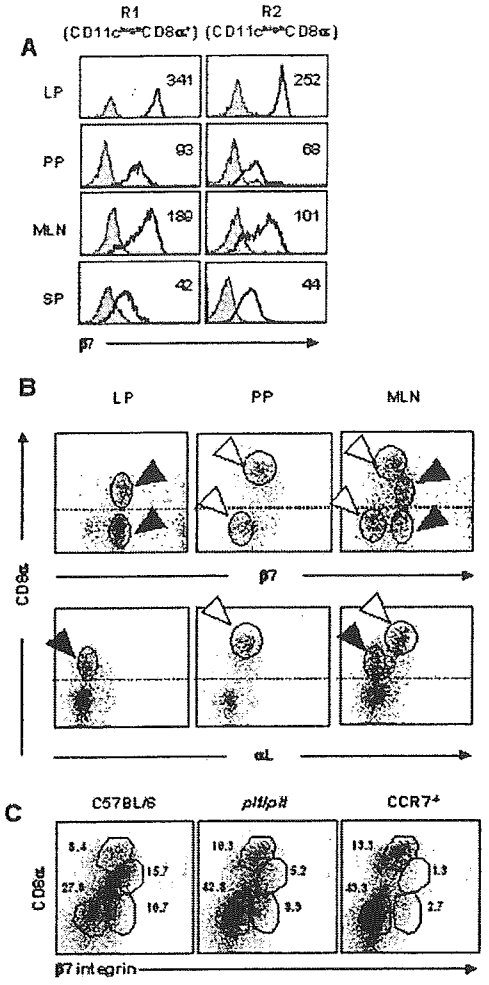

FIGURE 3. Apparent CCR7 dependency of the $CD8\alpha^{int}\beta_7^{high}$ and $CD8\alpha^-\beta_7^{high}$ subsets in MLNs. *A*, LP-DCs highly expressed β_7 integrin compared with other DCs. Low density cells from the LP were stained for CD11c, CD8α, and β_7 integrin, and the histogram profiles were acquired after gating on $CD11c^{high}CD8\alpha^+$ DCs (R1) or $CD11c^{high}CD8\alpha^-$ DCs (R2). ▨, Isotype controls; □, stained cells. The numbers in the histograms indicate the MFI. *B*, LP-DCs and PP-DCs appear to constitute the MLN-DCs. Low density cells from the LP were double stained for CD8α/integrin β_7 or for CD8α/integrin α_L. FACS profiles were acquired after gating on the $CD11c^{high}$ cells. Based on the CD8α/integrin β_7 double staining, the MLN-DCs consisted of four recognizable subsets, with two of them phenotypically corresponding to LP-DCs (filled arrowheads) and the remaining two corresponding to PP-DCs (open arrowheads). A similar observation was made with CD8α/integrin α_L double staining; MLN-DCs showed two $CD8\alpha^+$ subsets, one of which corresponded phenotypically to an LP-DC subset (filled arrowhead) and the other to a PP-DC subset (open arrowhead). *C*, $CD8\alpha^{int}\beta_7^{high}$ and $CD8\alpha^-\beta_7^{high}$ LP-DCs were significantly fewer in the MLNs of *plt/plt* mice and were almost absent from the MLNs of CCR7-deficient mice. Numbers indicate the percentage of each subset within gated $CD11c^{high}$ cells.

R2 subsets, respectively, and the PP-DCs had $CD8\alpha^{high}\beta_7^{int}$ and $CD8\alpha^-\beta_7^{low}$ populations. In contrast, the MLN-DCs contained all four surface phenotypes, supporting the possibility that LP-DCs and PP-DCs enter the MLNs to make up the four different DC subsets there (Fig. 3*B*). Furthermore, the examination of α_L expression in $CD8\alpha^+$ DCs revealed that those in the LP expressed relatively low levels of α_L ($CD8\alpha^{int}\alpha_L^{low}$), whereas those in PPs expressed high levels of α_L ($CD8\alpha^{high}\alpha_L^{high}$), and the MLN-DCs consisted of both populations (Fig. 3*B*). These observations thus suggest that the MLNs collect phenotypically different DCs from the LP and PPs, in accordance with the MLNs being the draining LNs of the LP and PPs.

We next asked whether these intestinal DCs enter the draining MLNs in a manner dependent on CCR7. For this purpose, we examined MLN-DCs in wild-type C57BL/6 mice; in C57BL/6-*plt/plt* mice, which are deficient in CCL19/CCL21-Ser (22); and in CCR7-deficient mice (21) that had been backcrossed to the C57BL/6 genetic background. As shown in Fig. 3*C*, the $CD8\alpha^{int}\beta_7^{high}$ and $CD8\alpha^-\beta_7^{high}$ subsets (R1 and R2 in the LP, respectively) represented subsets of the MLN-DCs of wild-type mice (15.7 and 10.7% of the total $CD11c^{high}$ DCs, respectively), but these subsets were significantly less prominent (5.2 and 8.9%) in the MLNs of *plt/plt* mice, which lack CCL21-Ser, but express CCL21-Leu, in their lymphatics, and were almost totally absent (1.3 and 2.7%) in the MLNs of CCR7-deficient mice. These results strongly suggest that both the R1 and R2 LP-DC subsets migrate to the MLNs in a CCR7-dependent manner under steady-state conditions. Consistent with this, both these LP-DC subsets were present in the intestine of CCR7-deficient mice (M. H. Jang and N. Sougawa, unpublished observation).

We also found that the majority of MLN-DCs were $CCR7^+$, as evidenced by their binding of a CCL19 fusion protein (Fig. 2*B*), and like the unique DCs documented in rat intestinal lymph by Huang et al. (15), MLN-DCs contained much debris in the cytoplasm (Fig. 4*A*). The pieces of debris were TUNEL positive, that is, they showed apoptosis-induced DNA fragmentation (Fig. 4*B*). In addition, a considerable proportion of these cells contained granules that were positive for alkaline phosphatase (Fig. 4*C*), which is expressed in epithelial cells, but not DCs. In contrast, the MLN-DCs themselves showed little phagocytic activity, as described below. These results are compatible with the idea that the $CCR7^+$ MLN-DCs were derived from the LP in a CCR7-dependent manner, after having ingested apoptotic IECs in the LP.

LP-DCs efficiently endocytose apoptotic epithelial cells

Because IECs undergo apoptosis extensively in situ, and because the DCs containing apoptotic epithelial cells are found in mesenteric lymph (15), we examined whether LP-DCs are unique in their ability to take up apoptotic IECs by observing isolated LP-DCs by transmission electron microscopy. As shown in Fig. 4*D*, the cytoplasm of the R1 cells contained numerous inclusions of 1–1.5 μm in diameter with membranous materials inside them, suggesting that these cells have a high phagocytic activity for apoptotic cells. The cytoplasm of the R2 subset contained fewer, but nonetheless distinct, phagocytic vesicles, a conspicuous Golgi network, well-developed rough endoplasmic reticulum, and numerous round mitochondria, suggesting that R2 is less phagocytic, but more active in protein synthesis and secretion, than R1. Both subsets showed a few finger-like protrusions from the cell body, with the protrusions from R2 cells being finer than those from R1 cells. These observations indicate that LP-DCs are highly active in the metabolism and phagocytosis of apoptotic cells.

Consistent with the above findings, in vitro analysis showed that both LP-DC subsets were highly phagocytic, efficiently and vigorously taking up CFSE-labeled apoptotic IECs (Fig. 4*E*), with the R1 subset taking up these cells more avidly than the R2 subset, as evidenced by conspicuous IEC-associated fluorescence staining in the cytoplasm (Fig. 4*F*). PP-DCs were heterogeneous in their phagocytic activity, with the $CD11b^-$ fraction of the population taking up apoptotic cells efficiently, and the $CD11b^+$ population showing less activity. In contrast, the MLN-DCs had little phagocytic activity regardless of their CD11b expression, and $CD11b^-$ SP-DCs showed intermediate levels of phagocytosis.

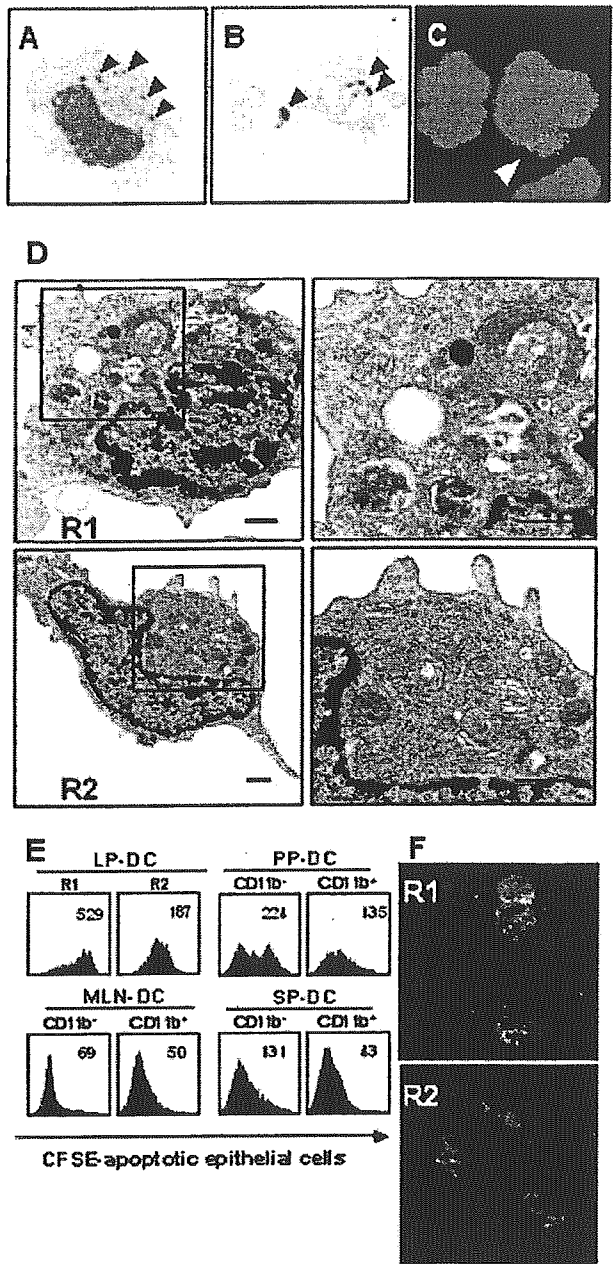

FIGURE 4. LP-DC subsets efficiently endocytose apoptotic IECs. *A–C*, The cytoplasm of MLN-DCs bearing the unique LP-DC phenotype contains cellular debris and fragmented DNA. *A*, FACS-sorted $CD11c^{high}CD8\alpha^{int}\alpha_L{}^{low}\beta_7{}^{high}$ MLN-DC stained with May-Grunwald-Giemsa shows abundant cellular debris in the cytoplasm. *B*, Two $CD11c^{high}CD8\alpha^{int}\alpha_L{}^{low}\beta_7{}^{high}$ MLN-DCs show TUNEL-positive inclusions. *C*, A $CD11c^{high}CD8\alpha^{int}\alpha_L{}^{low}\beta_7{}^{high}$ MLN-DC shows alkaline phosphatase-positive inclusions in the cytoplasm. *D*, Representative transmission electron microscopic views of cells from the LP-DC R1 (*upper*) and R2 (*lower*) subsets. All bars = 1 μm. *E*, Enriched DCs were cocultured with CFSE-labeled apoptotic IECs for 4 h. The DCs were then collected and stained for CD11c and CD11b and analyzed by flow cytometry. The numbers in the histograms indicate the MFI. *F*, Confocal microscopic images showing the uptake of CFSE-labeled apoptotic IECs by LP-DCs.

LP-DCs presenting IEC-associated Ag induce the differentiation of IL-10- and IL-4-producing $CD4^+$ T cells

We next investigated whether LP-DCs could present Ag associated with apoptotic cells to T cells. For this purpose, freshly isolated IECs from the small intestine were intracellularly loaded with OVA by osmotic shock and then allowed to undergo apoptosis spontaneously. Subsequently, the OVA-loaded apoptotic IECs were cocultured with DCs for 4 h, and the Ag-pulsed DC subsets were subjected to cell sorting. The purified DCs were then cocultured with DO11.10 T cells for 6 days, and T cell proliferation was measured by CFSE dilution. As shown in Fig. 5*A*, both the LP-DC subsets induced vigorous T cell proliferation, whereas a subset of SP-DCs, $CD11b^-$ SP-DCs, which displayed moderate phagocytic activity, induced slightly less T cell proliferation than the LP-DCs. The $CD11b^+$ SP-DCs, which had much less phagocytic activity than the LP-DCs, induced only weak proliferation. These results show that LP-DCs can take up apoptotic cells and present cell-associated Ags to T cells more potently than splenic DCs.

Mucosal DCs from the PPs and lungs tend to induce Th2 responses in T cell priming assays (3, 32). We therefore addressed whether LP-DCs also show this tendency by examining the cytokine secretion of OVA TCR-transgenic $CD4^+$ T cells primed by LP-DCs that had been exposed to OVA-loaded apoptotic IECs. As shown in Fig. 5*B*, T cells primed by LP-DCs expressed significantly higher levels of IL-4 and IL-10 than did SP-DC-primed T

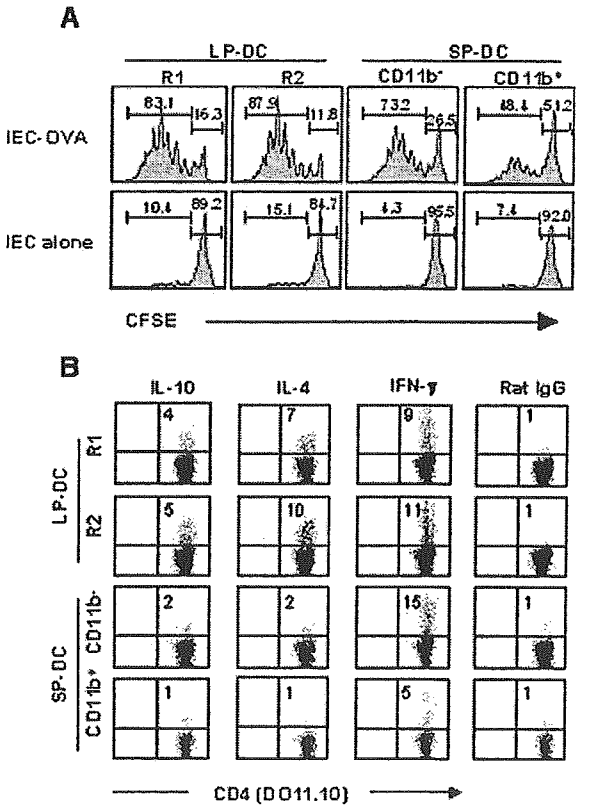

FIGURE 5. LP-DC subsets present IEC-associated Ags. *A*, LP-DC subsets induced cell-associated, Ag-specific T cell proliferation. Freshly isolated IECs were intracellularly loaded with OVA by osmotic shock, then allowed to undergo apoptosis spontaneously. LP-DCs were cocultured with the apoptotic IECs for 4 h, and the DCs were sorted using a FACSVantage SE. Subsequently, purified DCs bearing the OVA-containing IECs were cultured with naive DO11.10 T cells for 6 days. *B*, The LP-DCs primed DO11.10 T cells to produce IL-4 and IL-10. DCs bearing OVA-containing IECs were then cultured with DO11.10 T cells for 14 days (two rounds of stimulation with a 7-day interval). For intracellular cytokine staining, the T cells were restimulated with the anti-CD3ϵ mAb for 6 h in the presence of monensin. The data are representative of three independent experiments. Numbers within a quadrant indicate the percentage of cytokine-producing cells.

cells. The production of IFN-γ was comparable among the T cells primed with the different DCs. These results indicate that LP-DCs have a propensity to induce IL-4- and IL-10-producing T cells when exposed to Ag associated with apoptotic IECs.

Discussion

In this study we showed that there are at least two LP-DC subsets in the intestinal LP of unperturbed mice, and they both require CCR7 for their constitutive migration to MLNs. As speculated previously (15), LP-DCs can, in fact, present Ag associated with apoptotic IECs to naive $CD4^+$ T cells to induce the differentiation of IL-4- and IL-10-producing T cells. These observations indicate that LP-DCs with unique immunomodulatory activities migrate to MLNs in a CCR7-dependent manner to engage in the presentation of IEC-associated Ags from apoptotic IECs that were phagocytosed locally; this may help explain how a noninflammatory immune response can be maintained in MLNs under steady-state conditions.

Although it is generally accepted that DC migration is largely under the control of chemokines and chemokine receptors, studies of the molecules responsible for the migration of LP-DCs to MLNs in the steady state are lacking. The almost complete absence of DCs bearing the LP-DC phenotype ($CD11c^{high}CD8\alpha^{int}\beta_7{}^{high}$ and $CD11c^{high}CD8\alpha^-\beta_7{}^{high}$) in the MLNs of CCR7-deficient mice and their marked reduction in the MLNs of *plt/plt* mice, as shown in this study, provide strong evidence that CCR7 is critically important for LP-DC migration to the MLNs. Our unpublished observation that LP-DCs were found in the intestines of CCR7-deficient mice also supports this hypothesis. The ligands for CCR7 are CCL19 and CCL21. The *plt/plt* mouse strain congenitally lacks the expression of CCL19 and CCL21-Ser, but does express another CCL21 gene product, CCL21-Leu, in lymphatic endothelial cells (20). Thus, our data point to a critical role for CCR7-mediated signaling at the step of DC entry into the intestinal lymphatics, although additional investigation is required to pinpoint the site(s) of action of CCR7-mediated signaling. A pivotal role for CCR7 in the migration of skin DCs to afferent dermal lymphatics has been indicated in a report by Ohl et al. (23).

CCR7-mediated signaling may also play a role in the maturation and survival of LP-DCs transported to the MLNs, because CCR7 has been shown to induce antiapoptotic signaling (33) and terminal activation (34) in DCs. Although this issue could, in theory, be investigated by comparing the fate of CCR7-deficient vs wild-type LP-DCs within MLNs upon their injection into the intestinal lymphatics, a technical difficulty involved in applying this procedure to the mouse has prevented us from performing such experiments.

It is of note that although LP-DCs appeared to be relatively immature, showing a $CD80^{low}CD86^{int}$MHC class $II^{low}CD40^{low}$ phenotype, they expressed CCR7 and functionally responded avidly to CCL21 like mature DCs (19, 35). Given that immature DCs, albeit CCR7 negative initially, up-regulate their CCR7 expression upon ingestion of opsonized apoptotic cells (36), it is tempting to speculate that LP-DCs acquire CCR7 expression through the ingestion of apoptotic IECs in situ.

In contrast to the LP-derived DCs, the number of PP-derived DCs ($CD8\alpha^{high}\beta_7{}^{int}$ and $CD8\alpha^-\beta_7{}^{low}$) was not lower in the MLNs of *plt/plt* and CCR7-deficient mice (Fig. 4), indicating that PP-DCs do not depend on CCR7 signaling for migration to the MLNs. Previous studies showed that different PP-DC subsets differentially express multiple chemokine receptors, including CCR1, CCR2, CCR5, CCR7, CCR9, and CCR10, with all the subsets expressing functional CCR7 (4, 37). Although PP-DCs may use CCR7-mediated signaling for their localization within PP microdomains, as suggested previously (4), our study indicates that PP-DCs depend on non-CCR7 ligand chemokine(s) for their steady-state migration to MLNs.

Although recent studies of murine LP-DCs have identified several distinct subsets, i.e., $CD11c^+CD8\alpha^-CD11b^+$ (14, 38), $CD11c^+CD8\alpha^-CD11b^-$ (11, 14), $CD11c^+CD8\alpha^+CD11b^-$, $CD11c^{int}CD8\alpha^-CD11b^+B220^+$ (14), and $CD11c^-CD11b^-$ (30), our data presented in this paper clearly showed that, among these groups, the major contributors are from two populations, i.e., $CD11c^{high}CD8\alpha^{int}CD11b^{low}\alpha_L{}^{low}\beta_7{}^{high}$ (R1) and $CD11c^{high}CD8\alpha^-CD11b^{high}\alpha_L{}^{low}\beta_7{}^{high}$ (R2), in unperturbed mice. We also observed $CD11c^{int}CD11b^{high}$ cells to be abundant in the LP, but we did not include them in our current analysis, because they appeared to be different from conventional DCs, with numerous cytoplasmic eosinophilic granules. There were also low numbers of DC-like cells in our LP cell population, but they constituted only a very small proportion of the cells compared with R1 and R2, and thus they were not analyzed in the current study.

The recently reported $CD11c^+CD8\alpha^-CD11b^-$ LP-DCs constitutively expressing the IL-12 p40 promoter (11) and APCs with the $CD11c^-CD11b^-$ phenotype that constitutively express CD70 (30) may have been among the cell populations we did not study. In addition, a recent study identified $CX3CR1^+$ LP-DCs that form dendrites through the IECs of the terminal ileum to sample bacteria in the lumen directly (10). Because these $CX3CR1^+$ LP-DCs are $CD11c^{high}CD11b^{high}$, they resemble the R2 subset of our analysis. However, our preliminary observation indicates that hardly any cells in the R2 subset were reactive with an anti-CX_3CR1 mAb (M. H. Jang and N. Sougawa, unpublished observation).

Previous reports by Huang et al. (15) using mesenteric lymphadenectomized rats showed a DC subset in the intestinal lymph that constitutively transports apoptotic IECs to the T cell areas in MLNs. Our study demonstrated that although MLN-DCs with the LP-DC phenotype are poorly phagocytic, there is irrefutable evidence of previous phagocytosis, inasmuch as they contain much intracytoplasmic cellular debris, and both $CD8\alpha^{int}$ and $CD8\alpha^-$ LP-DC subsets can ingest apoptotic IECs vigorously and present IEC-associated Ag to $CD4^+$ T cells in vitro. These results strongly indicate that MLN-DCs containing considerable cellular debris correspond to the cells identified in the intestinal lymph by Huang et al. (15), and that the site of apoptotic cell acquisition by these cells is the LP.

Our observation that LP-DCs could polarize $CD4^+$ T cell differentiation to favor IL-4- and IL-10-producing T cells subsequent to coculture with Ag-loaded apoptotic IECs parallels the observation by Iwasaki and Kelsall (3) that PP-DCs generate T cells that produce high levels of IL-4 and IL-10 and less IFN-γ, as well as the observation by Alpan et al. (39) that Ag-loaded DCs present in MLNs can induce T cells to produce IL-4 and IL-10. Thus, certain intestinal DCs, including the LP-DCs, may have a tendency to induce Th2, rather than Th1, cells, which may be, at least in part, related to their localization to a specific microenvironment. Because phagocytosis of apoptotic cells has been reported to result in an anti-inflammatory state via transcriptional suppression of IL-12 (40), DCs that are closely colocalized with IECs in the LP may become locally imprinted not to induce Th1 cells upon ingestion of apoptotic IECs. In addition, conditioned medium of IECs have been shown to induce DCs to release IL-6 and to prime Th2 responses (41). Thus, the local microenvironment appears to confer on DCs a propensity to induce Th2 cells.

Collectively, these data provide strong evidence that CCR7 is critical for the recruitment of LP-DCs into the MLNs under steady-state conditions. Because these LP-DCs phagocytose apoptotic IECs and present IEC-associated Ag to induce IL-4- and IL-10-producing $CD4^+$ T cells, they are likely to be involved in the

immunomodulation of T cells within the MLNs. Thus, our study strengthens the idea that CCR7 is involved in the maintenance of peripheral tolerance (23) and points to a role for CCR7 in the recruitment of immunomodulatory DCs to the MLNs.

Acknowledgments

We thank Drs. S. Ono, H. Nakano, Y. Takahama, K. Matsushima, K. Hieshima, and O. Yoshie for providing valuable reagents and/or animals, and Dr. H. Hayasaka for critical reading of the manuscript. We also thank S. Yamashita and M. Komine for secretarial assistance, and Y. Nakano for technical help.

Disclosures

The authors have no financial conflict of interest.

References

1. Banchereau, J., F. Briere, C. Caux, J. Davoust, S. Lebecque, Y. J. Liu, B. Pulendran, and K. Palucka. 2000. Immunobiology of dendritic cells. *Annu. Rev. Immunol.* 18: 767–811.
2. Kelsall, B. L., and M. Rescigno. 2004. Mucosal dendritic cells in immunity and inflammation. *Nat. Immunol.* 5: 1091–1095.
3. Iwasaki, A., and B. L. Kelsall. 1999. Freshly isolated Peyer's patch, but not spleen, dendritic cells produce interleukin 10 and induce the differentiation of T helper type 2 cells. *J. Exp. Med.* 190: 229–239.
4. Iwasaki, A., and B. L. Kelsall. 2000. Localization of distinct Peyer's patch dendritic cell subsets and their recruitment by chemokines macrophage inflammatory protein (MIP)-3α, MIP-3β, and secondary lymphoid organ chemokine. *J. Exp. Med.* 191: 1381–1394.
5. Iwasaki, A., and B. L. Kelsall. 2001. Unique functions of CD11b$^+$, CD8α^+, and double-negative Peyer's patch dendritic cells. *J. Immunol.* 166: 4884–4890.
6. Kelsall, B. L., and W. Strober. 1996. Distinct populations of dendritic cells are present in the subepithelial dome and T cell regions of the murine Peyer's patch. *J. Exp. Med.* 183: 237–247.
7. Mora, J. R., M. R. Bono, N. Manjunath, W. Weninger, L. L. Cavanagh, M. Rosemblatt, and U. H. Von Andrian. 2003. Selective imprinting of gut-homing T cells by Peyer's patch dendritic cells. *Nature* 424: 88–93.
8. Iwata, M., A. Hirakiyama, Y. Eshima, H. Kagechika, C. Kato, and S. Y. Song. 2004. Retinoic acid imprints gut-homing specificity on T cells. *Immunity* 21: 527–538.
9. Rescigno, M., M. Urbano, B. Valzasina, M. Francolini, G. Rotta, R. Bonasio, F. Granucci, J. P. Kraehenbuhl, and P. Ricciardi-Castagnoli. 2001. Dendritic cells express tight junction proteins and penetrate gut epithelial monolayers to sample bacteria. *Nat. Immunol.* 2: 361–367.
10. Niess, J. H., S. Brand, X. Gu, L. Landsman, S. Jung, B. A. McCormick, J. M. Vyas, M. Boes, H. L. Ploegh, J. G. Fox, et al. 2005. CX_3CR1-mediated dendritic cell access to the intestinal lumen and bacterial clearance. *Science* 307: 254–258.
11. Becker, C., S. Wirtz, M. Blessing, J. Pirhonen, D. Strand, O. Bechthold, J. Frick, P. R. Galle, I. Autenrieth, and M. F. Neurath. 2003. Constitutive p40 promoter activation and IL-23 production in the terminal ileum mediated by dendritic cells. *J. Clin. Invest.* 112: 693–706.
12. Fagarasan, S., and T. Honjo. 2004. Regulation of IgA synthesis at mucosal surfaces. *Curr. Opin. Immunol.* 16: 277–283.
13. Fagarasan, S., K. Kinoshita, M. Muramatsu, K. Ikuta, and T. Honjo. 2001. In situ class switching and differentiation to IgA-producing cells in the gut lamina propria. *Nature* 413: 639–643.
14. Chirdo, F. G., O. R. Millington, H. Beacock-Sharp, and A. M. Mowat. 2005. Immunomodulatory dendritic cells in intestinal lamina propria. *Eur. J. Immunol.* 35: 1831–1840.
15. Huang, F. P., N. Platt, M. Wykes, J. R. Major, T. J. Powell, C. D. Jenkins, and G. G. MacPherson. 2000. A discrete subpopulation of dendritic cells transports apoptotic intestinal epithelial cells to T cell areas of mesenteric lymph nodes. *J. Exp. Med.* 191: 435–444.
16. Chung, Y., J. H. Chang, M. N. Kweon, P. D. Rennert, and C. Y. Kang. 2005. CD8α^-11b$^+$ dendritic cells but not CD8α^+ dendritic cells mediate cross-tolerance toward intestinal antigens. *Blood* 106: 201–206.
17. Chan, V. W., S. Kothakota, M. C. Rohan, L. Panganiban-Lustan, J. P. Gardner, M. S. Wachowicz, J. A. Winter, and L. T. Williams. 1999. Secondary lymphoid-tissue chemokine (SLC) is chemotactic for mature dendritic cells. *Blood* 93: 3610–3616.
18. Dieu, M. C., B. Vanbervliet, A. Vicari, J. M. Bridon, E. Oldham, S. Ait-Yahia, F. Briere, A. Zlotnik, S. Lebecque, and C. Caux. 1998. Selective recruitment of immature and mature dendritic cells by distinct chemokines expressed in different anatomic sites. *J. Exp. Med.* 188: 373–386.
19. Sallusto, F., P. Schaerli, P. Loetscher, C. Schaniel, D. Lenig, C. R. Mackay, S. Qin, and A. Lanzavecchia. 1998. Rapid and coordinated switch in chemokine receptor expression during dendritic cell maturation. *Eur. J. Immunol* 28: 2760–2769.
20. von Andrian, U. H., and T. R. Mempel. 2003. Homing and cellular traffic in lymph nodes. *Nat. Rev. Immunol.* 3: 867–878.
21. Forster, R., A. Schubel, D. Breitfeld, E. Kremmer, I. Renner-Muller, E. Wolf, and M. Lipp. 1999. CCR7 coordinates the primary immune response by establishing functional microenvironments in secondary lymphoid organs. *Cell* 99: 23–33.
22. Gunn, M. D., S. Kyuwa, C. Tam, T. Kakiuchi, A. Matsuzawa, L. T. Williams, and H. Nakano. 1999. Mice lacking expression of secondary lymphoid organ chemokine have defects in lymphocyte homing and dendritic cell localization. *J. Exp. Med.* 189: 451–460.
23. Ohl, L., M. Mohaupt, N. Czeloth, G. Hintzen, Z. Kiafard, J. Zwirner, T. Blankenstein, G. Henning, and R. Forster. 2004. CCR7 governs skin dendritic cell migration under inflammatory and steady-state conditions. *Immunity* 21: 279–288.
24. Kellermann, S. A., S. Hudak, E. R. Oldham, Y. J. Liu, and L. M. McEvoy. 1999. The CC chemokine receptor-7 ligands 6Ckine and macrophage inflammatory protein-3β are potent chemoattractants for in vitro- and in vivo-derived dendritic cells. *J. Immunol.* 162: 3859–3864.
25. Kanegasaki, S., Y. Nomura, N. Nitta, S. Akiyama, T. Tamatani, Y. Goshoh, T. Yoshida, T. Sato, and Y. Kikuchi. 2003. A novel optical assay system for the quantitative measurement of chemotaxis. *J. Immunol. Methods* 282: 1–11.
26. Yamamoto, M., K. Fujihashi, K. Kawabata, J. R. McGhee, and H. Kiyono. 1998. A mucosal intranet: intestinal epithelial cells down-regulate intraepithelial, but not peripheral, T lymphocytes. *J. Immunol.* 160: 2188–2196.
27. Haan, J. d., S. Lehar, and M. Bevan. 2000. CD8$^+$ but not CD8$^-$ dendritic cells cross-prime cytotoxic T cells in vivo. *J. Exp. Med.* 192: 1685–1696.
28. Yokota, Y., A. Mansouri, S. Mori, S. Sugawara, S. Adachi, S. Nishikawa, and P. Gruss. 1999. Development of peripheral lymphoid organs and natural killer cells depends on the helix-loop-helix inhibitor Id2. *Nature* 397: 702–706.
29. Nakano, H., M. Yanagita, and M. D. Gunn. 2001. CD11c$^+$B220$^+$Gr-1$^+$ cells in mouse lymph nodes and spleen display characteristics of plasmacytoid dendritic cells. *J. Exp. Med.* 194: 1171–1178.
30. Laouar, A., V. Haridas, D. Vargas, X. Zhinan, D. Chaplin, R. A. van Lier, and N. Manjunath. 2005. CD70$^+$ antigen-presenting cells control the proliferation and differentiation of T cells in the intestinal mucosa. *Nat. Immunol.* 6: 698–706.
31. Ardavin, C. 2003. Origin, precursors and differentiation of mouse dendritic cells. *Nat. Rev. Immunol.* 3: 582–590.
32. Akbari, O., R. H. DeKruyff, and D. T. Umetsu. 2001. Pulmonary dendritic cells producing IL-10 mediate tolerance induced by respiratory exposure to antigen. *Nat. Immunol.* 2: 725–731.
33. Sanchez-Sanchez, N., L. Riol-Blanco, G. de la Rosa, A. Puig-Kroger, J. Garcia-Bordas, D. Martin, N. Longo, A. Cuadrado, C. Cabanas, A. L. Corbi, et al. 2004. Chemokine receptor CCR7 induces intracellular signaling that inhibits apoptosis of mature dendritic cells. *Blood* 104: 619–625.
34. Marsland, B. J., P. Battig, M. Bauer, C. Ruedl, U. Lassing, R. R. Beerli, K. Dietmeier, L. Ivanova, T. Pfister, L. Vogt, et al. 2005. CCL19 and CCL21 induce a potent proinflammatory differentiation program in licensed dendritic cells. *Immunity* 22: 493–505.
35. Yanagihara, S., E. Komura, J. Nagafune, H. Watarai, and Y. Yamaguchi. 1998. EBI1/CCR7 is a new member of dendritic cell chemokine receptor that is up-regulated upon maturation. *J. Immunol.* 161: 3096–3102.
36. Verbovetski, I., H. Bychkov, U. Trahtemberg, I. Shapira, M. Hareuveni, O. Ben-Tal, I. Kutikov, O. Gill, and D. Mevorach. 2002. Opsonization of apoptotic cells by autologous iC3b facilitates clearance by immature dendritic cells, down-regulates DR and CD86, and up-regulates CC chemokine receptor 7. *J. Exp. Med.* 196: 1553–1561.
37. Zhao, X., A. Sato, C. S. Dela Cruz, M. Linehan, A. Luegering, T. Kucharzik, A. K. Shirakawa, G. Marquez, J. M. Farber, I. Williams, et al. 2003. CCL9 is secreted by the follicle-associated epithelium and recruits dome region Peyer's patch CD11b$^+$ dendritic cells. *J. Immunol.* 171: 2797–2803.
38. Anjuere, F., C. Luci, M. Lebens, D. Rousseau, C. Hervouet, G. Milon, J. Holmgren, C. Ardavin, and C. Czerkinsky. 2004. In vivo adjuvant-induced mobilization and maturation of gut dendritic cells after oral administration of cholera toxin. *J. Immunol.* 173: 5103–5111.
39. Alpan, O., G. Rudomen, and P. Matzinger. 2001. The role of dendritic cells, B cells, and M cells in gut-oriented immune responses. *J. Immunol.* 166: 4843–4852.
40. Kim, S., K. B. Elkon, and X. Ma. 2004. Transcriptional suppression of interleukin-12 gene expression following phagocytosis of apoptotic cells. *Immunity* 21: 643–653.
41. Rimoldi, M., M. Chieppa, V. Salucci, F. Avogadri, A. Sonzogni, G. M. Sampietro, A. Nespoli, G. Viale, P. Allavena, and M. Rescigno. 2005. Intestinal immune homeostasis is regulated by the crosstalk between epithelial cells and dendritic cells. *Nat. Immunol.* 6: 507–514.